ELSEVIER

Earth and Planetary Science Letters 126 (1994) 399–410

EPSL

# Viscosity and thickness of the asthenosphere detected from the Fennoscandian uplift

W. Fjeldskaar

*Rogaland Research, PO Box 2503, 4004 Stavanger, Norway*

Received 30 December 1993; revision accepted 17 June 1994

**Abstract**

The earth's response to the deglaciation in Fennoscandia is modelled using a layered viscous model with an elastic lithosphere. The modelled tilting of palaeoshorelines at particular locations peripheral to the former ice load and the pattern of the present rate of uplift consistent with the observations strongly suggest a low-viscosity asthenosphere. Earth models without a low-viscosity asthenosphere give significant mismatch to the present rate of uplift, and are unable to mimic the observed tilting of palaeoshorelines. Models with a viscosity of the lower mantle of $1.0–2.0 \times 10^{21}$ Pa s, and a viscosity of the upper mantle of $0.7–1.0 \times 10^{21}$ Pa s overlain by low-viscosity asthenosphere with a thickness ranging from 25 to 100 km, fit equally well with the observations. It is suggested strongly that the asthenosphere has a thickness of less than 150 km and a viscosity of less than $7.0 \times 10^{19}$ Pa s.

## 1. Introduction

Data on post-glacial uplift provide important information on the physical properties of the earth's mantle and lithosphere. Data from the Fennoscandian elevation of past shorelines and the present rate of uplift relative to sea level have been used with geophysical models to determine the physical properties of the earth's upper layers for many years [1]. There is, however, little agreement regarding the importance of the asthenosphere. Some have argued that a low-viscosity asthenosphere is needed to explain the pattern of uplift in Fennoscandia. As early as 1935 Van Bemmelen and Berlage [2] analyzed the Fennoscandian uplift and found that their data suggested a 100 km thick asthenosphere with a viscosity of $1.3 \times 10^{19}$ Pa s. McConnell [3] showed that the uplift data for Fennoscandia were consistent with a 200 km thick asthenosphere with a viscosity of the order of $10^{20}$ Pa s. Cathles [4,5], also based on Fennoscandian uplift data, argued strongly for a 75 km thick asthenosphere with a viscosity of $4 \times 10^{19}$ Pa s. Wolf [6] suggested that the asthenosphere is 100 km thick and has a viscosity of $1.2 \times 10^{19}$ Pa s. Some recent investigations, however, find no evidence of a low-viscosity asthenosphere [7–9]. In two previous studies [10,11] it has been shown, by the use of a maximum glaciation model, that the observed present uplift pattern cannot be explained satisfactorily without introducing a low-viscosity asthenosphere. Mitrovica and Peltier [12] have shown, with an inversion method, that the

[UC]

0012-821X/94/$07.00 
*SSDI* 0012-821X(94)00137-N

Fennoscandian uplift data give a non-unique solution to the mantle viscosity. Models with a weak asthenosphere overlying a $10^{21}$ Pa s deeper mantle provide a good fit to the Fennoscandian relaxation spectrum. This fit is also good with a low-viscosity zone lying above a two-layer deep mantle. In contrast to this conclusion the present study shows that the solution is unique, and that the uplift rate and palaeoshoreline tilts cannot be explained by models without a low-viscosity asthenosphere. The present study aims at placing a more stringent constraint on the asthenospheric

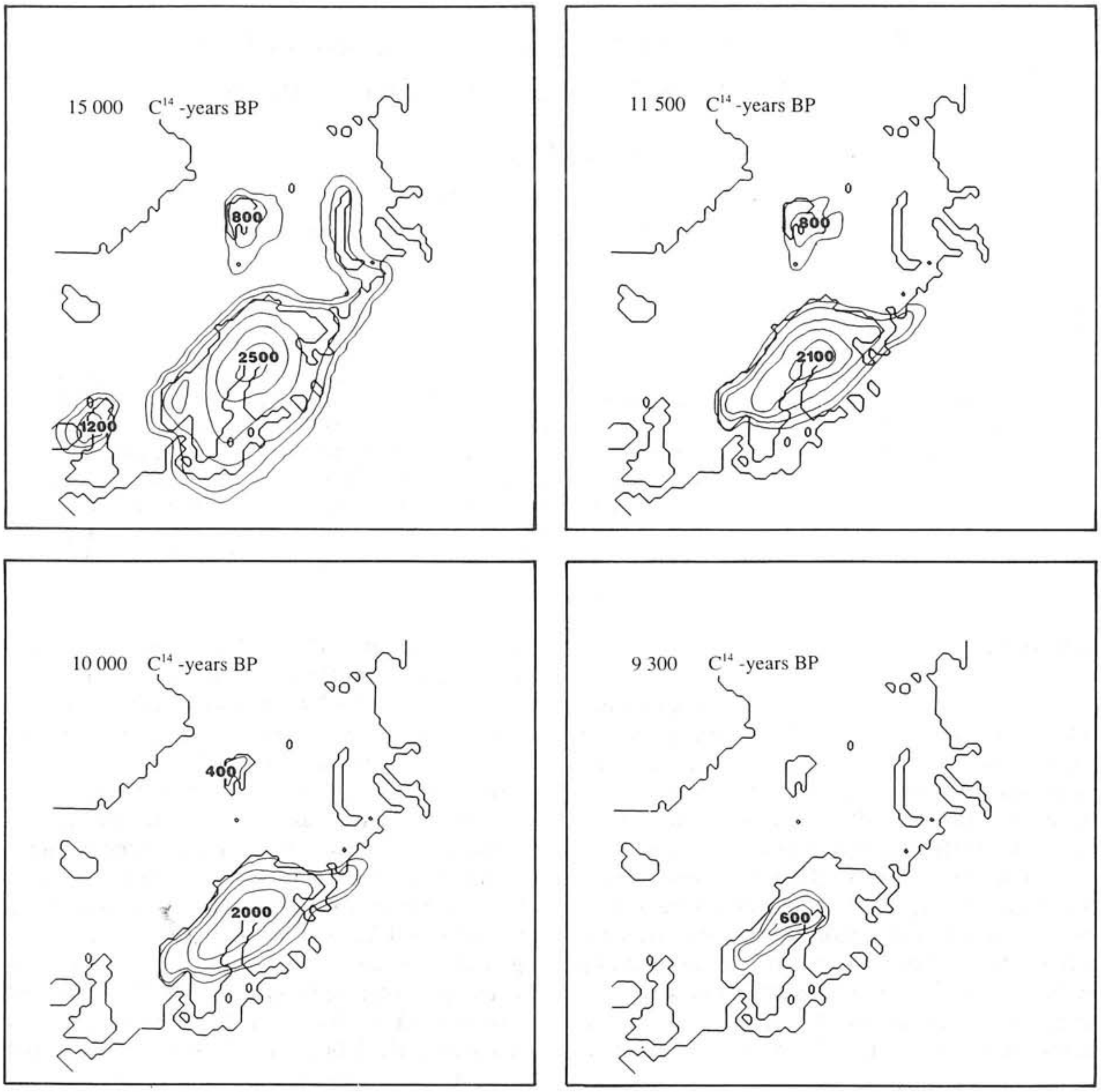


Fig. 1. The modelled extent and thickness of the ice sheet during the deglaciation in Fennoscandia (partly based on [27]). The contour interval is 400 m, except for the first 800 m. The contour interval for the ice sheet of 9300 yr BP is 200 m, except for the first 400 m.

thickness of Fennoscandia, and uses data from the more marginal parts of the Fennoscandian glaciation because this is where the critical data for clear determination of the mantle viscosity are found [4]. It is shown in a series of comparative calculations that changes in the asthenospheric thickness and viscosity have a significant impact on the present rate of uplift and tilting of the palaeoshorelines.

## 2. Modelling

The deglaciation history used in the calculations (Fig. 1) is different from that of the previous studies because it assumes an ice-free North Sea and Barents Sea at maximum glaciation. The extent of the ice sheet must be considered as a minimum. The ice thickness, however, is debatable, and the thickness used here must be considered as a maximum thickness. In a recent paper an argument for much thinner ice has been put forward [13]. The deglaciation model has been digitized with a spatial resolution of approximately 50 km by 50 km.

The earth is modelled as a half-space with constant gravitation and adiabatic density gradients in a Newtonian mantle in which the viscosity may vary with depth. The viscous fluid is overlain by an elastic lithosphere of constant thickness. With this flat earth model, the isostatic problem is treated analytically using the Fourier transform technique [4,10,11]. It has been shown that the errors introduced into the flexural response by a flat earth model are negligible [14,15]. The parameters used in the calculations are given in Table 1.

Table 1
Parameter values

| | |
|---|---|
| Young´s modulus | $8.35 \times 10^{10}$ Nm$^{-2}$ |
| Lame´s modulus | $3.34 \times 10^{10}$ Nm$^{-2}$ |
| Poisson´s ratio | 0.25 |
| Density of mantle | 3300 kg m$^{-3}$ |
| Density of glacier ice | 917 kg m$^{-3}$ |

## 3. Uplift data

This study uses two types of uplift data: present rate of uplift, and shoreline tilt vs. time. These processes are mainly the result of movement of the solid earth, and they are barely affected by movement of the sea level. Movements of the solid earth are here assumed to have a glacial isostatic origin connected with the melting of the last ice sheets. The uncertainties in the determination of the two data types are described in the below. In addition to the uncertainties in the determination, which can be quantified, there is also another uncertainty which cannot be quantified. This uncertainty is connected with the mechanism responsible for the observed movements. It is not unreasonable to assume that there is a neotectonic component in the uplift rate and the palaeoshoreline gradients [16,17]. At present, however, it is impossible to quantify this component. In this paper it is assumed that the neotectonism is of minor importance. The general pattern of the uplift is here believed to be the result of glacial isostasy, but there may be local disturbancies to this general pattern caused by tectonic processes.

## 4. Observed present rate of uplift

The observed present rate of uplift in Scandinavia relative to mean sea level [18] increases from 0 mm/yr on the coast of Norway to 9 mm/yr in central Sweden (Fig. 2). The uncertainty in the observations inland can be significant: near the coast and close to mareographs the standard error is at its best 0.2 mm/yr [19]. To obtain the uplift of the crust relative to the earth's centre rather than relative to mean sea level, the uplift rate must be corrected for eustatic changes. This involves (1) a correction for the gravitational effect of the uplift (geoidal eustasy) and (2) a correction for the uniform eustatic sea level change. The geoid change caused by ongoing redistribution of material within the earth is cal-

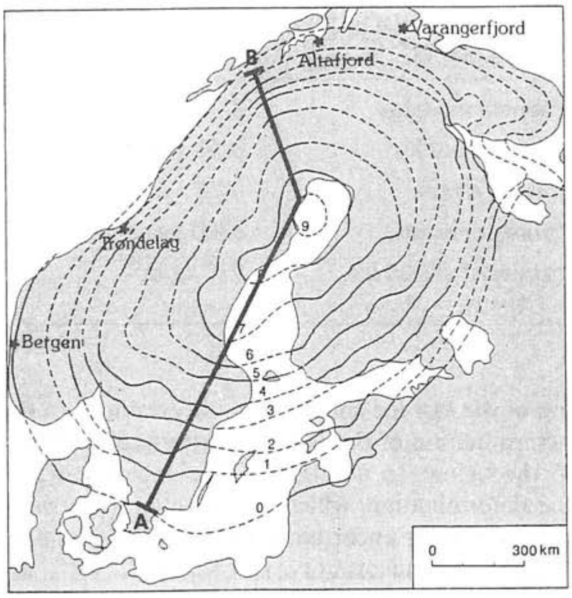


Fig. 2. Observed apparent rate of uplift in Fennoscandia [18]. Solid lines indicate areas covered by observations. The heavy line A–B indicates the position of the profile used to quantify the misfit between the observed and the theoretical rate of uplift (cf. Figs. 4 and 5).

culated at approximately 0.5 mm/yr in the central Baltic Sea [11]. There is no absolute measure of the global uniform eustatic change, and it is not an observable entity [20]. The closest we can come to an estimate is probably weighted averages from all the tide gauge data in the world, which show that the global sea level has risen by 1 mm/yr over the last century [21]. The uplift of the crust relative to the earth's centre is thus the sum of the present rate of uplift and the eustatic factors. Crustal uplift thus adds up to 1 mm/yr along the Norwegian coast and close to 10.5 mm/yr in central Fennoscandia.

## 5. Hydroisostasy

Hydroisostasy, the movement of the ocean bottom caused by sea level change, is modelled separately with the modelling technique described above. The land–ocean distribution during the deglaciation is assumed to be as present. For the modelled sea level change, assumed to take place outside the present land area, the published eustatic curve by Shepard [22] is used. The present rate of uplift/subsidence caused by this sea level rise is modelled as 0.0–0.2 mm/yr along the Norwegian coast, and as −0.2 to +0.2 mm/yr along the eastern coast of Sweden (Fig. 3). This is, however, a simplification, because the water loads will never be distributed uniformly over the oceans. The significance of spatially non-uniform water loads in post-glacial relative sea level has been specifically addressed in a recent paper [23]. However, it is evident from the modelling (Fig. 3) that the hydroisostatic effect of uniform (as well as non-uniform) water loads does not have a significant impact on the pattern of the present rate of uplift in Fennoscandia.

## 6. Theoretical present rate of uplift

During the modelling the maximum present uplift rate is kept close to 10 mm/yr (matching the observations) by adjusting the viscosity profile. A series of earth models with viscosity profiles which give a present uplift rate of 10 mm/yr is shown in Table 2. The uplift patterns in the

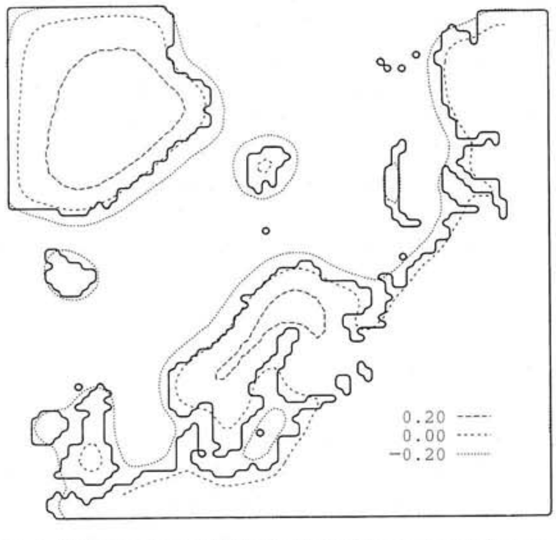


Fig. 3. Calculated present hydroisostatic movements (mm/yr) caused by the eustatic sea level change according to Shepard [22]. Earth model used in the calculations is model 4 (Table 2).

peripheral areas will be different for different mantle viscosity profiles. In most cases a flexural rigidity of $10^{23}$ N m (elastic thickness $t_e = 24$ km) is used, which is assumed to be at the lower end of that considered realistic.

Previous modelling shows that the observed uplift pattern cannot be explained satisfactorily without introducing a low-viscosity asthenosphere [11]. The best-fit model for the maximum glaciation model was obtained with a mantle viscosity of $1.0 \times 10^{21}$ Pa s and a 75 km asthenosphere with a viscosity of $1.3 \times 10^{19}$ Pa s. The modelled asthenosphere rheology was exactly the same as that proposed by Van Bemmelen and Berlage in 1935 [2], and in accords with the conclusion of Wolf [6]. Mitrovica and Peltier [12] conclude that this model does not fit with the Fennoscandian relaxation spectrum. Their conclusion is based on a relaxation spectrum for our best-fit model (model LVZ, fig. 11 in [12]) with relaxation times exceeding 6000 yr. It is, however, shown in [10] that the maximum relaxation time for this earth rheology is 3800 yr. The correct relaxation spectrum gives an excellent fit to the Fennoscandian relaxation spectrum presented in [12].

In the following we shall examine different mantle rheologies (Table 2) in terms of present rate of uplift, modelled on the basis of the above-mentioned deglaciation history and sea level history.

*Mantle viscosity below $1.0 \times 10^{21}$ Pa s*: We shall start our examination of the different viscosity profiles with a uniform mantle. The one and only uniform mantle viscosity that theoretically gives a present-day maximum rate of uplift of 10 mm/yr is $0.54 \times 10^{21}$ Pa s. The deviations from the observed present rate of uplift are significant, up to 4 mm/yr in central parts of the profile

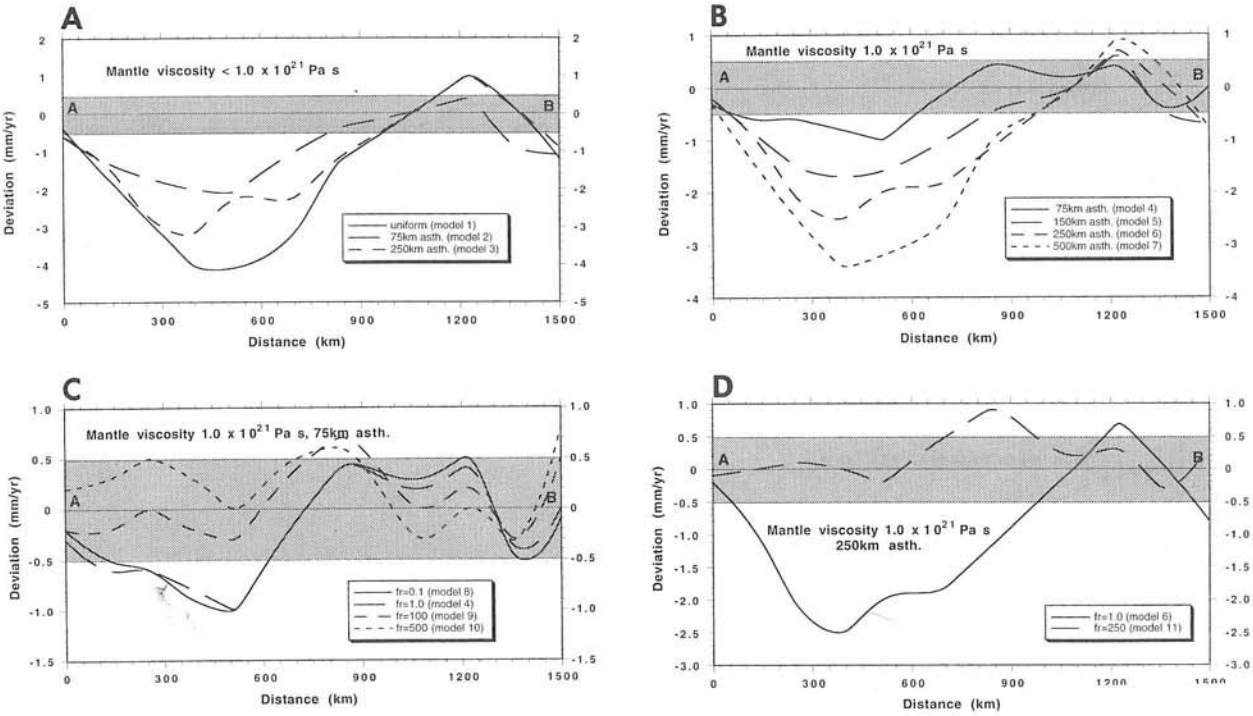


Fig. 4. Deviations between observed and theoretical present rate of uplift on a profile across Fennoscandia (for location, see Fig. 2). (A) Models with mantle viscosity of less than $1.0 \times 10^{21}$ Pa s (models 1–3, Table 2). (B) Models with mantle viscosity of $1.0 \times 10^{21}$ Pa s, and changing asthenospheric thickness (models 4–7). (C) Models with mantle viscosity of $1.0 \times 10^{21}$ Pa s, and changing flexural rigidities (models 4 and 8–10). (D) Models with mantle viscosity of $1.0 \times 10^{21}$ Pa s, thick asthenosphere and changing flexural rigidities (models 6 and 11). The shaded area represents the assumed error of the observed present rate of uplift (0.5 mm/yr).

(Fig. 4A). Introducing a low-viscosity asthenosphere above a mantle with a viscosity of $0.8 \times 10^{21}$ Pa s reduces the deviations, especially for models with a thin asthenosphere. However, the deviations from the observations nevertheless remain significant, indicating that the earth's mantle has a viscosity above $0.8 \times 10^{21}$ Pa s.

*Mantle viscosity of $1.0 \times 10^{21}$ Pa s*: The next series of calculations is for a mantle with a of viscosity of $1.0 \times 10^{21}$ Pa s (Fig. 4B). The model with a thin asthenosphere (75 km) gives a better fit to the observations than a thicker asthenosphere (150–500 km). For a thin asthenosphere the maximum deviations are reduced to half compared with the mantle with a viscosity of $0.8 \times 10^{21}$ Pa s. For models with a thin asthenosphere changes in the flexural rigidity cause only minor adjustments (Fig. 4C). The deviations between the observations and models with a thick asthenosphere, however, can be reduced by increasing the lithosphere rigidity (Fig. 4D). Thus, a thick asthenosphere combined with a high rigidity lithosphere gives a good fit. As will be shown later, however, this is not a viable option, because models with high flexural rigidity cannot produce the observed palaeoshoreline gradients.

*Lower mantle with a viscosity of $2.0 \times 10^{21}$ Pa s*: The next series of calculations is carried out with a mantle that has a viscosity of $2.0 \times 10^{21}$ Pa s overlain by a low-viscosity asthenosphere. Models with an asthenosphere thinner than 250 km give significantly higher uplift rates in the periphery than is observed (Fig. 5A). However, for models with a very thick low-viscosity asthenosphere (or, rather, an upper mantle with a lower viscosity) the long-wavelength components decay fast enough to reduce the peripheral uplift rate. This suggests that a model with a lower mantle

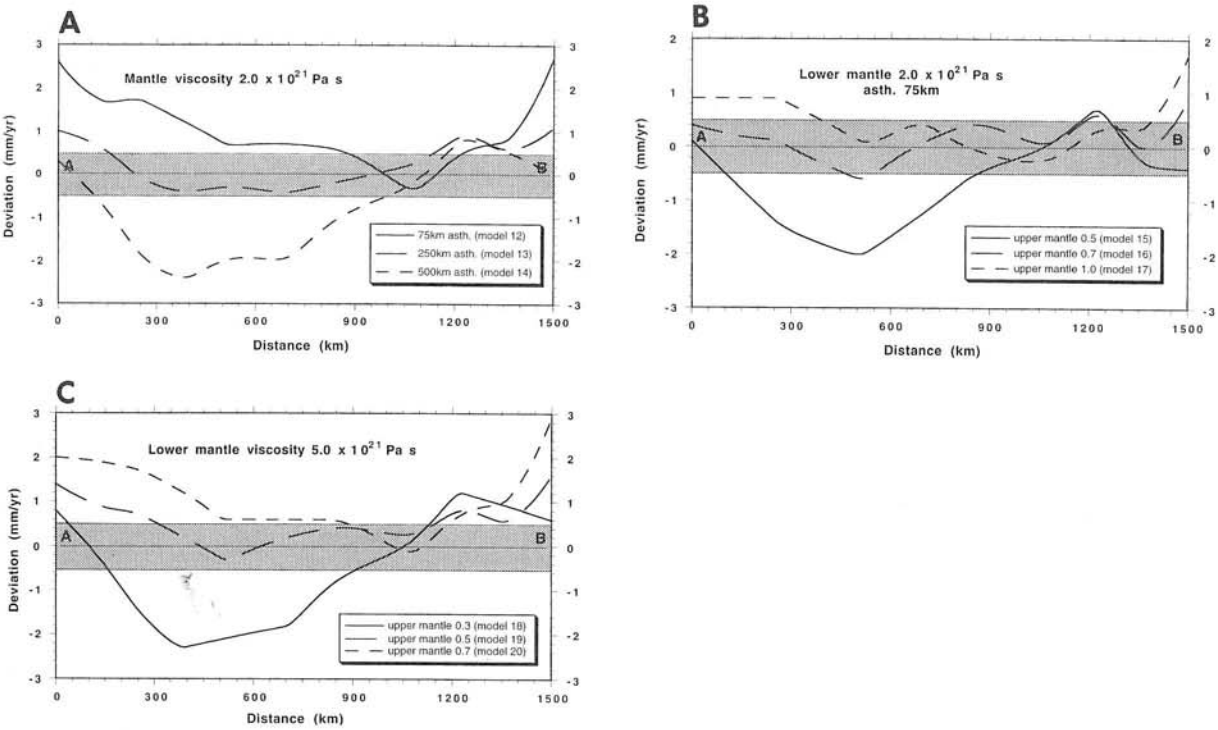


Fig. 5. Deviations between observed and theoretical present rate of uplift on a profile across Fennoscandia (for location, see Fig. 2). (A) Models with mantle viscosity of $2.0 \times 10^{21}$ Pa s, and changing asthenospheric thickness (models 12–14, Table 2). (B) Models with lower mantle viscosity of $2.0 \times 10^{21}$ Pa s, a 75 km low-viscosity asthenosphere and changing upper mantle viscosity (models 15–17). (C) Models with lower mantle viscosity of $5.0 \times 10^{21}$ Pa s, and changing upper mantle viscosity (models 18–20). The shaded area represents the assumed error of the observed present rate of uplift (0.5 mm/yr).

Table 2
Rheological models

| Model no. | Lower mantle viscosity $10^{21}$ Pa s | Upper mantle viscosity $10^{21}$ Pa s | Asthenosphere thickness km | Asthenosphere viscosity $10^{19}$ Pa s | Lithosphere Flexural rigidity $10^{23}$ Nm |
|---|---|---|---|---|---|
| 1 | 0.54 | 0.54 | -- | -- | 1.0 |
| 2 | 0.8 | 0.8 | 75 | 2.0 | 1.0 |
| 3 | 0.8 | 0.8 | 250 | 24.0 | 1.0 |
| 4 | 1.0 | 1.0 | 75 | 1.4 | 1.0 |
| 5 | 1.0 | 1.0 | 150 | 7.0 | 1.0 |
| 6 | 1.0 | 1.0 | 250 | 17.5 | 1.0 |
| 7 | 1.0 | 1.0 | 500 | 38.0 | 1.0 |
| 8 | 1.0 | 1.0 | 75 | 1.4 | 0.1 |
| 9 | 1.0 | 1.0 | 75 | 2.0 | 100.0 |
| 10 | 1.0 | 1.0 | 75 | 10.0 | 500.0 |
| 11 | 1.0 | 1.0 | 250 | 40.0 | 250.0 |
| 12 | 2.0 | 2.0 | 75 | 0.65 | 1.0 |
| 13 | 2.0 | 2.0 | 250 | 11.0 | 1.0 |
| 14 | 2.0 | 2.0 | 500 | 29.0 | 1.0 |
| 15 | 2.0 | 0.5 | 75 | 2.8 | 1.0 |
| 16 | 2.0 | 0.7 | 75 | 1.45 | 1.0 |
| 17 | 2.0 | 1.0 | 75 | 0.96 | 1.0 |
| 18 | 5.0 | 0.33 | -- | -- | 1.0 |
| 19 | 5.0 | 0.5 | 75 | 1.7 | 1.0 |
| 20 | 5.0 | 0.7 | 75 | 0.93 | 1.0 |

(below 670 km) viscosity of $2.0 \times 10^{21}$ Pa s overlain by an upper mantle of significantly lower viscosity could also fit the observations, if we introduce a low-viscosity asthenosphere that could remove the short-wavelength deviations in central parts of the profile.

Introducing a thin low-viscosity asthenosphere into models with a lower mantle viscosity of $2.0 \times 10^{21}$ Pa s gives a good fit if the upper mantle has a viscosity close to $0.7 \times 10^{21}$ Pa s. The fit is as good as for a lower mantle viscosity of $1.0 \times 10^{21}$ Pa s (model 4). An upper mantle with $0.5 \times 10^{21}$ Pa s or $1.0 \times 10^{21}$ Pa s gives a significantly worse fit to the observations (Fig. 5B).

*Lower mantle with a viscosity above $2.0 \times 10^{21}$ Pa s*: Models with a lower mantle with a viscosity higher than $2.0 \times 10^{21}$ Pa s give uplift rates in the peripheral areas that are too high (Fig. 5C). These high peripheral uplift rates cannot be reduced by increasing the flexural rigidity, as shown above, because such increases actually lead to higher uplift rates in the peripheral areas. It is difficult to imagine a lower flexural rigidity in the coastal areas of Norway, and even if such low flexural rigidity did hold sway, the effect on the present uplift rates would be minor (cf. models 4 and 8 in Fig. 4C).

*No low-viscosity asthenosphere*: Two recent investigations have, however, explained the Fennoscandian uplift without introducing a low-viscosity asthenosphere. One of them [7], based on global data, has a lower mantle with a viscosity of

$2.0 \times 10^{21}$ Pa s that is overlain by an upper mantle with a viscosity of $1.0 \times 10^{21}$ Pa s. However, application of the above glaciation history to this model gives a central uplift of more than 19 mm/yr. This can be reduced to 10 mm/yr by a considerable increase in the flexural rigidity (1.5 $\times 10^{26}$ N m, $t_e \approx 275$ km). It appears from the above results that the peripheral uplift rates for such a flexural rigidity value will be much too high [cf. 11]. An alternative to this high flexural rigidity is a reduction in the ice thickness. Theoretically this could also give a central uplift rate of 10 mm/yr. However, as will be shown later, a thinner ice will increase the misfit between the observed and theoretical palaeoshoreline tilting in western Norway. Peltier's model, which is based on an attempt to reconcile a global database, does not fit with the observations for Fennoscandia, and must be refined to include a low-viscosity asthenosphere, at least for this area.

The other model [8,9], based on data from northwest Europe, has an upper mantle viscosity of $3–5 \times 10^{20}$ Pa s and a lower mantle viscosity of $2–7 \times 10^{21}$ Pa s. Modelling the present rate of uplift with the above glaciation history and a lower mantle viscosity of $2 \times 10^{21}$ Pa s, for example, requires an upper mantle viscosity close to $3 \times 10^{20}$ Pa s to match the observed maximum rate of uplift. This model gives an uplift pattern across the profile similar to that of model 14 (Table 2 and Fig. 5A), which shows large deviations from the observations. Similar discrepancies are found for a lower mantle viscosity spanning from 2 to $7 \times 10^{21}$ Pa s.

In general, models with a lower mantle viscosity of $2.0 \times 10^{21}$ Pa s or higher, without a low-viscosity asthenosphere, are not viable options. The reason is that the short-wavelength components decay too slowly, giving significant deviations in central parts of the uplift dome.

Conclusions based on the present rate of uplift are as follows:

(1) The lower mantle has a viscosity $1.0 \times 10^{21}$ Pa s and not significantly more than $2.0 \times 10^{21}$ Pa s.

(2) The upper mantle viscosity is between 0.7 and $1.0 \times 10^{21}$ Pa s.

(3) The present rate of uplift in Fennoscandia is impossible to explain without introducing a low-viscosity asthenosphere. For models with mantle viscosity of $1.0 \times 10^{21}$–$2.0 \times 10^{21}$ Pa s any low-viscosity asthenospheric thickness between 25 and 150 km gives uplift patterns with a good fit to the observations, if the flexural rigidity is between 1.0 and $500.0 \times 10^{23}$ N m ($24 < t_e < 190$ km; Fig. 6A). Models with asthenospheric thickness above 150 km give a significant deviation from the observed present rate of uplift (Fig. 6B).

## 7. Tilting of palaeoshorelines

The post-glacial sea level changes in Fennoscandia have been mapped with shoreline diagrams, which show the displacement and tilting of the palaeoshorelines. Four sites along the coast of Norway with observed palaeoshoreline tilting have been selected for the present investigation. These are Bergen, Trøndelag, Altafjord and Varangerfjord (Fig. 2).

The accuracy of the shore level displacement data, on which the gradient curves are based, varies because different determination methods have been used. The curves from southern Norway have the highest accuracy, because they are based on dated cores from dammed lakes of different heights. The uncertainties could have three different sources [24]: (1) determination of the isolation contact, (2) determination of the threshold height, and (3) dating of the sediments. The uncertainty range for (1) is 1–2 cm and for (2) is less than 1 m. The most crucial point is the dating of the sediments. The uncertainty in radiocarbon dating is generally less than 200–300 yr [24]. The total uncertainty in the determination of the late-glacial gradients for Trøndelag and Bergen is thus probably less than 0.1 m/km.

Another uncertainty is, as mentioned above, the interpretation of the uplift curves. Significant parts of the tilts could, theoretically, be caused by neotectonism. There are post-glacial sea level observations from western Norway that clearly indicate tectonic movements [16]. However, it is assumed here that the tectonic influence on the curves used in this paper is of minor importance.

The calculations of the tilting history for our four sites (Fig. 7) have been carried out with the different mantle and lithosphere models given in Table 2 (models 4–6, 8, 9, 11, 14 and 19). The geoid change caused by uplift is not considered here, because the influence on the calculated tilts is insignificant [25], at less than 5 cm/km [26].

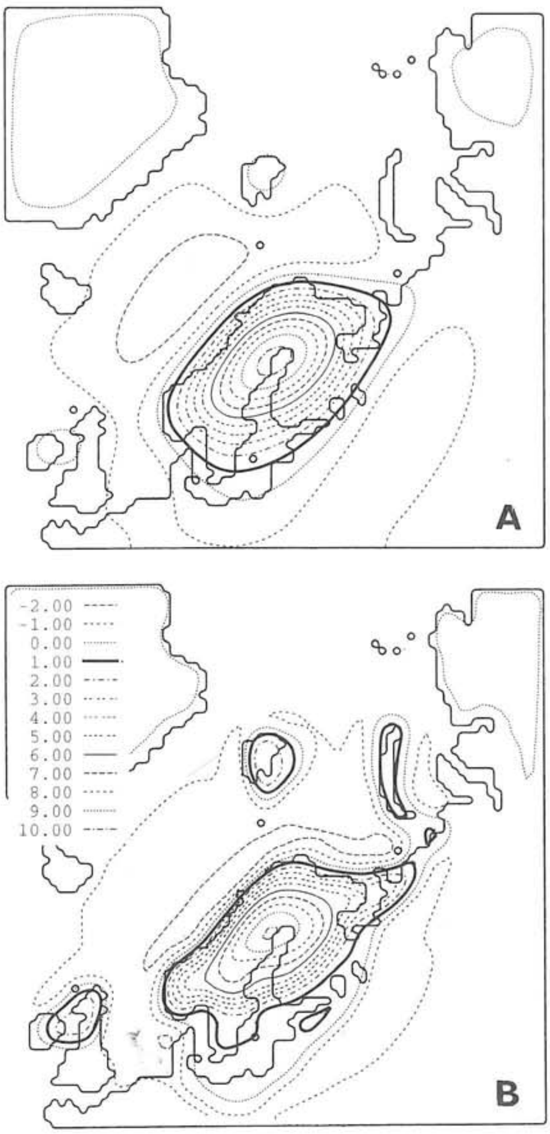


Fig. 6. Theoretical present rate of uplift (mm/yr). (A) $1.0 \times 10^{21}$ Pa s mantle with a 75 km thick asthenosphere. (B) $1.0 \times 10^{21}$ Pa s mantle with a 250 km thick asthenosphere (note the uneven uplift contour spacing in southern Sweden). Note also that the 1 mm/yr contour (the heavy solid line) corresponds to the zero contour of the observed apparent rate of uplift (Fig. 2).

The main results are as follows:

The gradient curves at the more peripheral locations (Altafjord and Varangerfjord, Figs. 7C and D) give a reasonably good fit with the observations assuming a thin (75 km) low-viscosity asthenosphere and a low flexural rigidity ($1.0 \times 10^{23}$ N m, $t_e \approx 24$ km). However, the same is the case for models with a thicker (250 km) asthenosphere combined with a higher flexural rigidity ($250 \times 10^{23}$ N m, $t_e \approx 150$ km). (Note that the modelling assumes an ice-free Barents Sea. The influence of a Barents Sea ice on these gradient curves depends on the ice thickness and the timing of the deglaciation, but in general it will tend to reduce the gradients at these locations, and in the Varangerfjord area in particular.) Despite this, models with a very thick asthenosphere (models 6 and 14) seem to be unrealistic, because they give palaeoshoreline tilts that are close to double the observed values (Altafjord).

The western Norway gradients (Bergen and Trøndelag, Figs. 7A and B) are clearly more sensitive to asthenospheric thickness and lithosphere rigidity than the northern Norway data. Models with an asthenosphere thicker than 250 km give gradients in late-glacial time that are too low, and too slow a gradient decay as a function of time. Models with flexural rigidity greater than $100 \times 10^{23}$ N m are also not in accordance with the observations, giving similar low gradients in late-glacial time. To obtain higher late-glacial gradients a thin asthenosphere combined with a low flexural rigidity is required. A model with a mantle that has a viscosity of $1.0 \times 10^{21}$ Pa s overlain by a 75 km low-viscosity asthenosphere with a flexural rigidity of $1.0 \times 10^{23}$ Nm gives late-glacial gradients that are slightly higher than those observed. These gradients could, however, be reduced by a minor increase in the flexural rigidity or in the asthenospheric thickness.

The models consistent with the tilting observations have a low-viscosity asthenosphere overlying an upper mantle with a viscosity of $0.5–1.0 \times 10^{21}$ Pa s. Any asthenospheric thickness between 25 and 100 km (with a viscosity between 0.06 and $2.7 \times 10^{19}$ Pa s) fit equally well with the observed

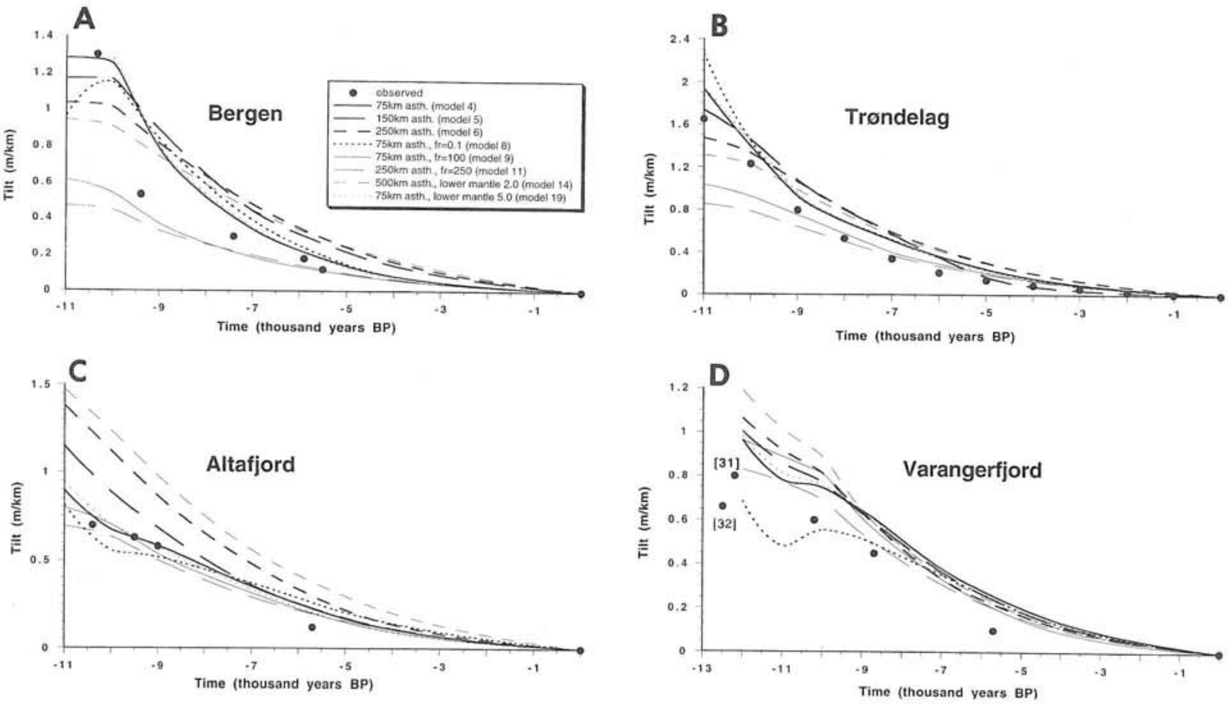


Fig. 7. Theoretical vs. observed shoreline tilting for (A) Bergen [28], (B) Trøndelag [24], (C) Altafjord [29,30] and (D) the Varangerfjord area (low gradient at ca. 12000 yr BP from [31], high gradient from [32]). Locations are shown in Fig. 2. Theoretical models are 4–6, 8, 9, 11, 14 and 19 (Table 2).

tilting histories. An asthenospheric thickness of more than 150 km (viscosity of $7.0 \times 10^{19}$ Pa s) introduces deviations from the observations.

Models without a low-viscosity asthenosphere, as proposed by Peltier [7] and Lambeck [8,9], will give gradients that are more or less similar to model 14 (Table 2, a lower mantle of $2.0 \times 10^{21}$ Pa s and a 500 km thick asthenosphere). It is clearly shown that this model is not a viable option, because it cannot produce the observed shoreline gradients. The palaeoshoreline gradients for model 14 are too high for sites farthest from the centre of the ice (northern Norway) (Figs. 7C and D) and too low tilts for sites closer to the centre of the ice (western Norway) (Figs. 7A and B), demonstrating that the misfit cannot be reduced by modification of the ice thickness. A thinner ice will give increased misfit between the observed and theoretical palaeoshoreline tilting in western Norway.

## 8. Conclusion

Models consistent with the observed present rate of uplift and palaeoshorelines in Fennoscandia strongly suggest that the earth's mantle has a low-viscosity asthenosphere. Published mantle models without a low-viscosity asthenosphere are unable to explain the uplift pattern. Models with a lower mantle viscosity of $1.0\text{–}2.0 \times 10^{21}$ Pa s, and an upper mantle viscosity of $0.7\text{–}1.0 \times 10^{21}$ Pa s overlain by a low-viscosity asthenosphere with a thickness ranging from 25 to 100 km, fit equally well with the observations. An asthenospheric thickness of 150 km gives significant deviations from the observations, strongly suggesting that the asthenosphere is in fact less than 150 km thick, with a viscosity of less than $7.0 \times 10^{19}$ Pa s. The modelling is carried out with an ice model with maximum ice thickness. A minor reduction in the ice thickness gives a minor increase in the modelled mantle viscosity. A significant reduction in the ice thickness seems to be out of the question because it gives an increased misfit between the observed and theoretical palaeoshoreline tilting.

## Acknowledgements

I thank the three anonymous referees for their constructive reviews of an earlier version of this paper.

## References

[1] M. Ekman, A concise history of postglacial land uplift research (from its beginning to 1950), Terra Nova 3, 358–365, 1991.

[2] R.W. van Bemmelen and H.P. Berlage, Versuch einer mathematischen Behandlung geotektonischer Bewegung unter besonderer Berucksichtegung der Undationstheorie, Beitr. Geophys. 43, 19–55, 1935.

[3] R.K. McConnell, Viscosity of the mantle from relaxation time spectra of isostatic adjustment, J. Geophys. Res. 73, 7089–7105, 1968.

[4] L.M. Cathles, The Viscosity of the Earth's Mantle, 386 pp., Princeton University Press, Princeton, N.J., 1975.

[5] L.M. Cathles, Interpretation of postglacial isostatic adjustment phenomena in terms of mantle rheology, in: Earth Rheology, Isostasy and Eustasy, N.A. Mörner, ed., pp. 11–45, Wiley, 1980.

[6] D. Wolf, An upper bound on lithosphere thickness from glacio-isostatic adjustment in Fennoscandia, J. Geophys. 61, 141–149, 1987.

[7] W.R. Peltier, Mechanisms of relative sea-level change and the geophysical responses to ice–water loading, in: Sea Surface Studies, R.J.N. Devoy, ed., pp. 57–95, Croom Helm, London, 1987.

[8] K. Lambeck, A model for Devensian and Flandrian glacial rebound and sea-level change in Scotland, in: Glacial Isostasy, Sea Level and Mantle Rheology, R. Sabadini, K. Lambeck and E. Boschi, eds, pp. 33–63, Kluwer, 1991.

[9] K. Lambeck, P. Johnston and M. Nakada, Holocene glacial rebound and sea-level change in NW Europe, Geophys. J. Int. 103, 451–468, 1990.

[10] W. Fjeldskaar and L. Cathles, Rheology of mantle and lithosphere inferred from post-glacial uplift in Fennoscandia, in: Glacial Isostasy, Sea Level and Mantle Rheology, R. Sabadini, K. Lambeck and E. Boschi, eds., pp. 1–19, Kluwer, 1991.

[11] W. Fjeldskaar and L. Cathles, The present rate of uplift of Fennoscandia implies a low-viscosity asthenosphere, Terra Nova 3, 393–400, 1991.

[12] J.X. Mitrovica and W.R. Peltier, The inference of mantle viscosity from an inversion of the Fennoscandian relaxation spectrum, Geophys. J. Int. 114, 45–62, 1993.

[13] A. Nesje and S.O. Dahl, Autochthonous block fields in southern Norway: implications for the geometry, thickness, and isostatic loading of the Late Weichselian Scandinavian ice sheet, J. Quat. Sci. 5, 225–234, 1990.

[14] D. Wolf. The relaxation of a spherical and flat Maxwell Earth models and effect due to the presence of a lithosphere, J. Geophys. 56, 24–33, 1984.

[15] F. Amelung and D. Wolf, Viscoelastic perturbations of the Earth: significance of the incremental gravitational force in models of glacial isostasy, Geophys. J. Int. 117, in press.

[16] K. Anundsen, Late Weichselian relative sea levels in southwest Norway: observed strandline tilts and neotectonic activity, Geol. Fören. Stockholm Förh. 111, 288–292, 1989.

[17] K. Anundsen and W. Fjeldskaar, Observed and theoretical Late Weichselian shore-level changes related to glacier oscillations at Yrkje, southwest Norway, in: Late and Postglacial Oscillations of Glaciers: Glacial and Periglacial Forms, H. Schroeder-Lanz, ed., pp. 133–170, Balkema, Rotterdam, 1983.

[18] M. Ekman, Impacts of geodynamic phenomena on systems for height and gravity, Bull. Geod. 63, 181–196, 1989.

[19] M. Ekman, Postglacial rebound and sea level phenomena, with special reference to Fennoscandia and the Baltic Sea, in: Geodesy and Geophysics, J. Kakkuri, ed., Publ. Finn. Geod. Inst. 115, 7–70, 1993.

[20] W. Fjeldskaar, Rapid eustatic changes—never globally uniform, in: Correlation in Hydrocarbon Exploration, J. Collinson, ed., pp. 13–19, Nor. Pet. Soc. and Graham and Trotman, 1989.

[21] V. Gornitz, S. Lebedev and J. Hansen. Global sea level trend in the past century, Science 215, 1611–1614, 1982.

[22] F.P. Shepard. Thirty-five thousand years of sea level, in: Essays on Marine Geology, T. Clements et al., eds., pp. 1–10, University of Southern California Press, 1963.

[23] P. Johnston, The effect of spatially non-uniform water loads on prediction of sea-level change, Geophys. J. Int. 114, 615–634, 1993.

[24] A. Kjemperud, Late Weichselian and Holocene shoreline displacement in the Trondheimsfjord area, central Norway, Boreas 15, 61–82, 1986.

[25] D. Wolf, On deglaciation-induced perturbations of the geoid, Can. J. Earth Sci. 23, 269–272, 1986.

[26] W. Fjeldskaar and R. Kanestrøm, Younger Dryas geoid deformation caused by deglaciation in Fennoscandia, in: Earth Rheology, Isostasy and Eustasy, N.A. Mörner, ed., pp. 569–574, Wiley, 1980.

[27] B.G. Andersen, Late Weichselian ice sheets in Eurasia and Greenland, in: The Last Great Ice Sheets, G.H. Denton and T.J. Hughes, eds., pp. 437–467, Wiley, 1981.

[28] P.E. Kaland, Holocene shore displacement and shorelines in Hordaland, western Norway, Boreas 13, 203–242, 1984.

[29] M. Marthinussen, Coast and fjord area of Finnmark, in: Geology of Norway, O. Holtedahl, ed., Nor. Geol. Unders. 215, 416–429, 1960.

[30] M. Marthinussen, $C_{14}$-datings referring to shoreline transgressions and glacial substages in Northern Norway, Nor. Geol. Unders. 215, 37–68, 1962.

[31] M. Marthinussen, Contributions to the Quaternary geology of northeasternmost Norway and the closely adjoining foreign territories, Nor. Geol. Unders. 315, 1–157, 1974.

[32] J.L. Sollid, S. Andersen, N. Hamre, O. Kjeldsen, O. Salvigsen, S. Sturød, T. Tveitå and A. Wilhelmsen, Deglaciation of Finnmark, north Norway, Nor. Geogr. Tidsskr. 27, 233–325, 1973.